16 Disordered and Biological Soft Matter

M. Ackermann, C.M. Aegerter, F. Atzeni, P. Dagenais (since September 2015), D. Dreher, D. Eder, A. Keller, F. Lanfranconi, A. Mallavalli, A. Pataki (Master student), S. Puri, R. Rüttimann (Master student), L. Schertel (since April 2015), J. Schneider, L. Selvaggi and S. Urdy

in collaboration with:
Institute of Molecular Life Sciences (K. Basler, T. Aegerter-Wilmsen, L. Pelkmans, D. Brunner), ETH Zürich (P. Koumoutsakos), MPI für Planzenforschung Köln (R.S. Smith), University of Fribourg (A. Jazwinska), University of Bern (C. Kulemeier, S. Robinson, P. Barbier de Reuille), Biozentrum Basel (M. Affolter), University of Konstanz (G. Aubry, G. Maret, T. Sperling), MPI für Selbstorganisation Göttingen (C.C. Maass), Deutsches Luft- und Raumfahrtzentrum (M. Sperl), University of Twente (A. Mosk), Université Joseph Fourier Grenoble (S. Skipetrov), Université Paris Denis Diderot (F. Graner), Technion Haifa (E. Akkermans).

The group of disordered and biological soft-matter, is interested in problems of disordered materials outside of thermal equilibrium, such that instabilities can arise that lead to the emergence of structures. Our specific investigations fall into three overarching themes: The first is concerned with light transport in disordered media, where the wave-nature of light leads to the emergence of a transition in transport, known as Anderson localization, which we have studied in detail. Furthermore we investigate the transport in turbid media with the development of novel imaging techniques. These are also useful in the second class of problems, the regulation of biological development via mechanical forces. The growth of the Drosophila wing and its folds or the regeneraton of fins of the zebrafish are used for this study. Finally, the control of developmental processes by mechanical forces is also studied in the morphogenetic process of dorsal closure in Drosophila embryos. To complement these biological systems, we are also studying purely physical non-equilibrium systems such as granular gases and foams in diamagnetic levitation to obtain overall properties of instabilities in disordered non-equilibrium systems.

In the last year, we have made progress in several of these areas, which are discussed in detail below. These subjects concern Anderson localization, imaging in turbid media, the growth of Drosophila wing imaginal discs as well as the application of minute forces to tissues in the Drosophila embryo via magnetic tweezers.

16.1 Anderson localization of light

When considering wave-transport in extremely disordered samples, where the scattering is strong enough to lead to a mean free path that is of the order of the wave length of light, Anderson predicted more than 50 years ago that a transition to localization of the waves can occur [1]. In spite of the age of this prediction, the experimental realization of an Anderson localization transition in three dimensions [2] still remains elusive and has lead to intense discussions in the research community [3–6]. We have studied this question in recent years in time resolved transmission data that show non-classical behavior, in that the width of the transmission profile shows a saturation [7] and the integrated time-of flight spectra show a sub-exponential tail [8–10], see Fig. 16.1.

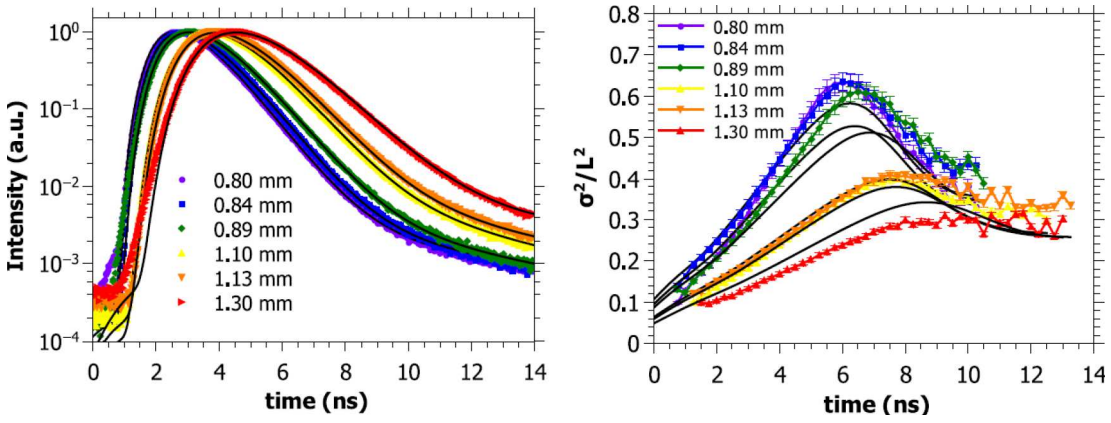

FIG. 16.1 – Time of flight (a) and time dependence of the transmission profile (b) of TiO_2 samples with different thickness showing non-classical diffusion.

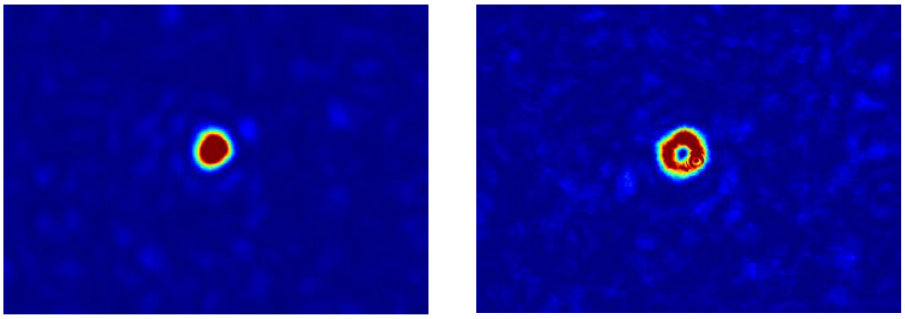

FIG. 16.2 – Wave-front shaping after optimization is used to produce a structured illumination with a wider angular imaging range in Fourier-space reaching up to 36 regularly spaced spots. The procedure allows to increase the spatial resolution of such an image by using several such illuminations akin to structured illumination microscopy.

However, studying samples of decreasing thickness as well as the wave-length dependence of these results has shown that additional processes can be at work, such as fluorescence [11]. With a time resolved spectral measurement and a theoretical model including time delayed fluorescence, we can completely describe the non-classical diffusion in these samples (black curves in Fig. 16.1) without invoking effects of Anderson localization [11].

[1] P.W. Anderson, Phys. Rev. **109**, 5 (1958).

[2] E. Abrahams *et al.*, Phys. Rev. Lett. **42**, 673 (1979).

[3] D.S. Wiersma, P. Bartolini, A. Lagendijk, *et al.*, Nature **390**, 671 (1997).

[4] F. Scheffold, R. Lenke, R. Tweer, *et al.*, Nature **398**, 206 (1999).

[5] F. Scheffold and D. Wiersma, Nature Photonics **7**, 933 (2013).

[6] G. Maret, T. Sperling, W. Bührer, M. Ackermann, A. Lubatsch, R. Frank, and C.M. Aegerter, Nature Photonics **7**, 934 (2013).

[7] T. Sperling, W. Bührer, C.M. Aegerter, and G. Maret, Nature Photonics **7**, 48 (2013).

[8] M. Störzer, P. Gross, C.M. Aegerter and G. Maret, Phys. Rev. Lett. **96**, 063904 (2006).

[9] C.M. Aegerter M. Störzer, and G. Maret, Europhys. Lett. **75**, 562 (2006).

[10] T. Sperling, W. Bührer, M. Ackermann, C.M. Aegerter, and G. Maret, New J. of Phys. **16**, 112001 (2014).

[11] T. Sperling, L. Schertel, M. Ackermann, G. Aubroy, C.M. Aegerter, and G. Maret, New J. of Phys. **18**, 013039 (2016).

16.2 Structured illumination using spatial light modulation

We used the principle of wave-front shaping to image structures behind turbid layers [12–14] to control the sample illumination [15]. The structured illumination is used as a reference sample to resolve structures beyond the wavelength of the light. For this purpose, we for instance change the focus after wave-front shaping to a doughnut shape, see Fig. 16.2.

With such an illumination in addition to the scanning of the focus, an edge enhancement of the structures can be achieved, which leads to a sharper image of the structure of interest [15], as illustrated in Fig. 16.3 for a single fluorescent particle of 500 nm diameter, which has been scanned

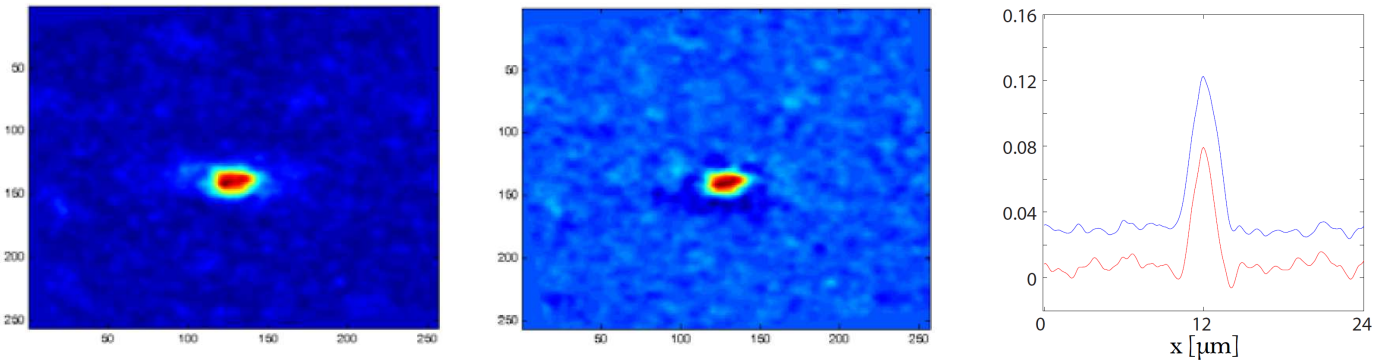

FIG. 16.3 – Using a doughnut-shaped beam to illuminate a fluorescent bead in addition to a focused beam can lead to an increase in sharpness of an image. Left: imaging with a scanning focus, middle: a combination of two images, obtained with a scanning focus as well as a scanning doughnut, right: cross-sections of the two images, red with, blue without scanning doughnut.

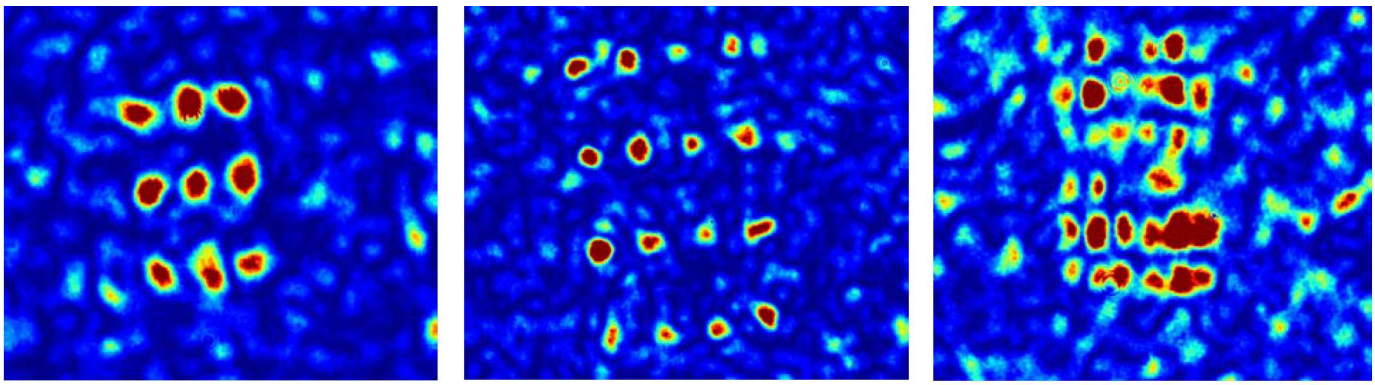

FIG. 16.4 – Wave-front shaping after optimization is used to produce a structured illumination with a wider angular imaging range in Fourier-space reaching up to nine (left), sixteen (middle) and up to 36 (right) regularly spaced spots. This points a way to increase the spatial resolution of such an image akin to structured illumination microscopy.

both with a focused as well as a doughnut-shaped beam. The difference of these two illuminations gives the center image showing a sharper outline of the bead, as indicated by the cross-section shown on the right [15]. We are in the process of extending these techniques of structured illumination for a possible application as a super-resolution microscope without tailored fluorophores or light sources. As has been discussed in [16, 17], such a superposition of incoming light with effectively two different wave vectors can lead to an increase in resolution beyond the Abbe limit in real space by a factor given by the number of wave vectors superposed.

The fact that there is an additional periodicity in the illumination, gives an additional intensity of the light emitted by the fluorophore, i.e. the sample in a shifted region of reciprocal space. The total wave-vector is then enlarged, leading to an increase in resolution in direct space. Another way to see this is that the comparison of a modulated periodic illumination (from the sample) with the unchanged periodic illumination gives a Moiré-pattern from which the modulating structure can be derived directly [16]. For this purpose, we are changing the focus formed by the wave-front shaping through the turbid layer into a range of multiple spots, which can then be used in conjunction with a reference image to increase the range of the image in Fourier space [18]. Examples are shown in Fig. 16.4, where a single spot has been distributed into nine, sixteen or 36 spots. This way it is possible to create a version of structured light illumination microcopy that does not rely on the alignment of several beams, but uses wave-front shaping instead.

[12] I. M. Vellekoop and C.M. Aegerter, Opt. Lett. **35**, 1245 (2010).

[13] G. Ghielmetti and C.M. Aegerter, Opt. Express **20**, 3744 (2012).

[14] G. Ghielmetti and C.M. Aegerter, Opt. Express **22**, 1981 (2014).

[15] G. Ghielmetti, PhD thesis, University of Zurich (2014).

[16] M.G.L. Gustafsson, Proc Natl Acad Sci U S A. **102**, 13081 (2005).

[17] J.T. Frohn, H.F. Knapp, and A. Stemmer, Proc Natl Acad Sci U S A. **97**, 7232 (2000).

[18] A. Malavalli, M. Ackermann, C.M. Aegerter, to be published (2016).

16.3 In-vivo imaging of Drosophila wing disc development

We have used a modification of a confocal microscope in conjunction with index matching of the cuticle to image the development of organs in the Drosophila larvae in order to study the additional information that can be gained using live imaging in turbid situations [19]. Two examples are presented here in more detail. The first example concerns a direct study of the time evolution of cell shapes in the wing disc in order to investigate the connection between cell proliferation and mechanical forces [20]. This has been put forward as a mechanism for the regulation of size in the wing disc [21–24], akin to the regulation of bone structure due to mechanical stresses [25]. Sample images of cell shapes at different time points in development are shown in Fig. 16.5. It can be seen that cells are well resolved and one can not only determine cell area, but also cell deformations and therefore one has a measure of forces acting on the cells at different times [20].

We have found that tension and cell proliferation are correlated during the growth of the wing disc. This has then also been corroborated by direct application of forces to the tissue, while simultaneously determining the proliferation rate.

In the second example, we have studied the positional information within the growing wing disc, see Fig. 16.6, by investigating the position and size of fluorescently labeled clones in the wing disc all through development [19, 26].

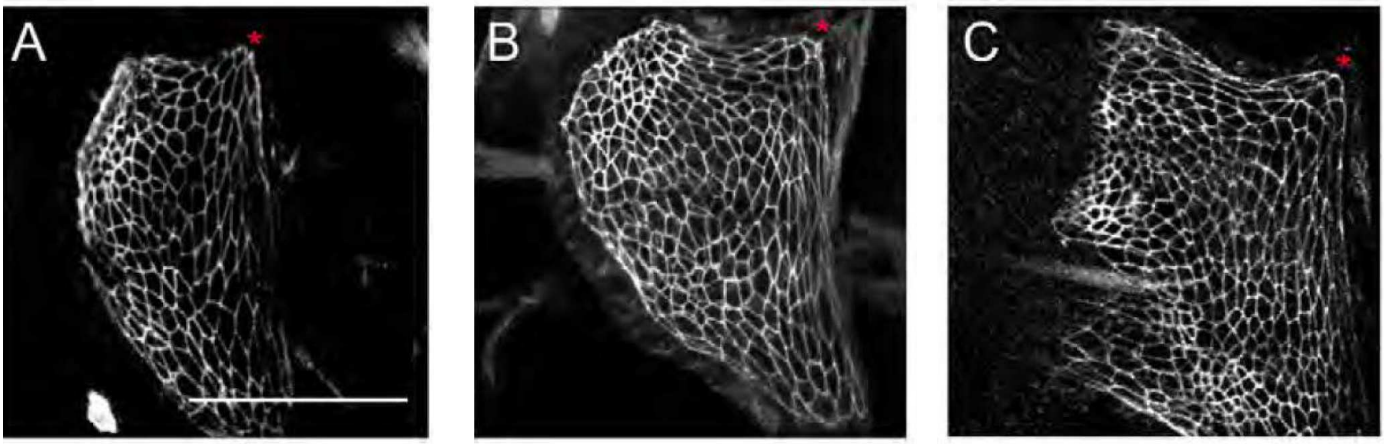

FIG. 16.5 – Fluorescent cell images in a developing wing imaginal disc after the second instar phase, allowing to determine the external forces exerted by a muscle fiber attached at the red asterisk and to study their effect on proliferation of the tissue. The scale bar corresponds to 50 μm.

This yields information on developmental boundaries as well as how differential growth rate lead to the overall shape of the tissue. Fig. 16.6 shows positional paths of several clones in two wing imaginal discs, where the initial position of the clones during the first instar is above (left) and below (right) the wing-notum boundary respectively [26]. To align the images of the different time steps during which the wing disc increases in size more than tenfold the attachment point of the muscle fibre, shown in Fig. 16.5, has been used as a reference point (see Fig. 16.6), since it presents an external point of reference [26].

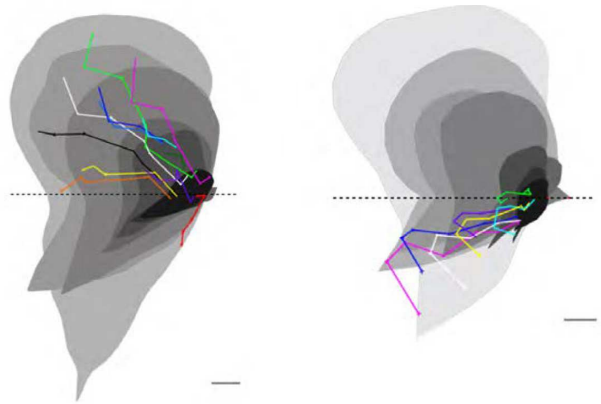

FIG. 16.6 – Time-dependent analysis of growth in two wing imaginal discs from the analysis of initially single cell clones. Using in-vivo imaging inside the Drosophila larva, it was possible to study the growth path of cells in the wing imaginal disc and therefore the shaping of the tissue due to proliferation. Aligning all time points on the attachment of the muscle fibre connecting the wing disc to the haltere, one can see that positions above and below the wing-notum boundary (dashed line) stay separated all through development. The scale bars correspond to 50 μm.

[19] U. Nienhaus, T. Aegerter-Wilmsen, and C.M. Aegerter, PLoS One **7**, e47594 (2012).

[20] T. Schluck, U. Nienhaus, T. Aegerter-Wilmsen, and C.M. Aegerter, PLoS One **8**, e76171 (2013).

[21] T. Aegerter-Wilmsen, C.M. Aegerter, E. Hafen, and K. Basler, Mechanisms of Development **124**, 318 (2007).

[22] L. Hufnagel *et al.*, Proc. Nat. Acad. Sci USA **104**, 3835 (2007).

[23] T. Aegerter-Wilmsen *et al.*, Development **139** 3221 (2012).

[24] U. Nienhaus, T. Aegerter-Wilmsen, and C.M. Aegerter, Mechanisms of Development **126**, 942 (2009).

[25] F.M. Lambers *et al.*, Bone **52**, 587 (2013).

[26] U. Nienhaus, PhD thesis, University of Zurich 2013.

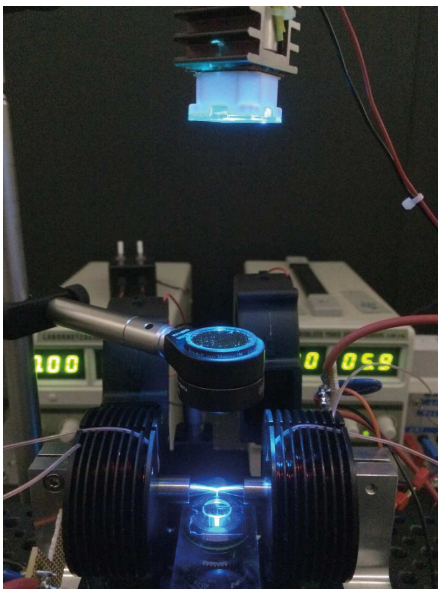

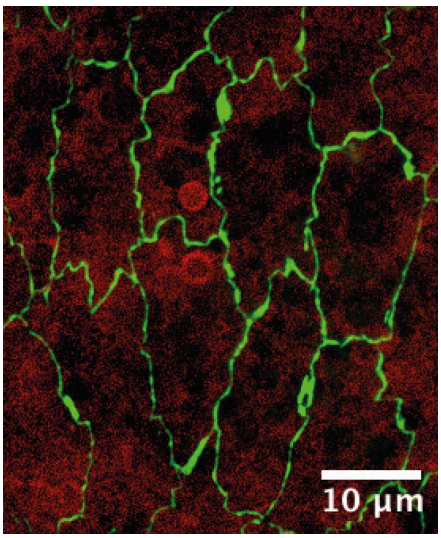

FIG. 16.7 – The magnetic tweezer setup and custom built fluorescence microscope is shown on the left. This magnetic tweezer is used to exert forces in AS tissues during dorsal closure in the embryonal development of Drosophila. As shown on the right, super-paramagnetic beads can be enclosed in AS cells, shown by green fluorescent protein-tagged Armadillo (GFP-Arm), a marker of the apical cell circumference. This will allow the application of forces of 100 pN to individual AS cells during development.

16.4 Magnetic tweezers for influencing tissue development in Drosophila embryos

We also investigate the process of dorsal closure in the Drosophila embryo [27], where mechanical forces lead to a generation of shape in the epidermal tissue of the Drosophila embryo. This happens by closing an opening in the tissue filled with large cells, called Amnioserosa (AS) cells, which during dorsal closure contract strongly, thus closing the opening in the epidermis.

In order to study the forces acting during that process, and to influence at the same time the mechanics of the process, we have built a magnetic tweezer setup [28]that allows to apply forces on individual super-paramagnetic beads of up to 200 pN. It was calibrated by determining the displacement speeds in a fluid of known viscosity. Using direct feedback in the application of the current to the magnetic tweezer, compressional as well as tension forces can be applied [29].

To allow to apply forces to AS cells during dorsal closure, the super-paramagnetic beads have to be inserted into these cells, which is possible to achieve using microinjection during early embryonic development as shown in Fig. 16.7. Here, the beads are seen inside the AS cells which are marked fluorescently.

[27] J. Solon, A. Kaya-Copur, J. Colombelli, and D. Brunner, Cell **137**, 1331-42 (2009).

[28] M. Tanasa, N. Biais, and M. Sheetz, Methods Cell Biol. **83**, 473-93 (2007).

[29] P.Kollmannsberger, B. Fabry, Rev. Sci. Inst. **78**, 114301 (2007).